DOI: 10.1002/chem.200601198

Dynamic Combinatorial Libraries Based on Hydrogen-Bonded Molecular Boxes

Jessica M. C. A. Kerckhoffs, Miguel A. Mateos-Timoneda, David N. Reinhoudt,* and Mercedes Crego-Calama*[a]

Abstract: This article describes two different types of dynamic combinatorial libraries of host and guest molecules. The first part of this article describes the encapsulation of alizarin trimer $\mathbf{2a}_3$ by dynamic mixtures of up to twenty different self-assembled molecular receptors together with the amplification and selection of the best binder. Receptors $(\mathbf{1a}–\mathbf{d})_3\cdot(DEB)_6$ are formed by the self-assembly of six diethyl barbiturate (DEB) and calix[4]arene dimelamine derivatives **1a–d** by using hydrogen bonds. The largest amplification factor (2.8) for a host assembly ($\mathbf{1a}_3\cdot(DEB)_6$) was observed after the addition of **2a** to four-component library $\mathbf{1a}_n\cdot\mathbf{1b}_{(3-n)}\cdot(DEB)_6$ ($n=0$–3). Addition of **2a** to twenty-component library $\mathbf{1a}_n\cdot\mathbf{1b}_m\cdot\mathbf{1c}_o\cdot\mathbf{1d}_{(3-(n+m+o))}\cdot(DEB)_6$ (n, m, $o=0$–3; $(n+m+o)\leq 3$) also showed amplification of receptor $\mathbf{1a}_3\cdot(DEB)_6$. The second part of this article describes the complexation of libraries of different alizarin-like guest molecules (**2a–d**) and the self-assembled receptor $\mathbf{1a}_3\cdot(DEB)_6$. This receptor is able to template the formation of the best-fitting guest trimer.

Keywords: binding selectivity · combinatorial chemistry · hydrogen bonds · molecular capsules · self-assembly

Introduction

Combinatorial chemistry (CC) can be seen as the process of diversity generation and it is now widely used in the search for biologically active compounds, new materials, and catalysts.[1] The combination of CC with supramolecular chemistry (self-assembly directed by molecular recognition) led to the new research field of dynamic combinatorial chemistry (DCC)[2] in which building blocks are connected to each other by means of reversible linkages.[3] These reversible linkages can be covalent, such as the imines reported by Lehn and Huc,[4] or the disulfides that were described by Otto et al.[5] Alternatively, the links can be noncovalent, as shown by the groups of Severin and Fujita who used metal–ligand coordination,[6] and by our group through the use of hydrogen bonds.[7] In recent years, examples of the combination of noncovalent interactions and dynamic covalent bonds have also appeared.[3b–g] DCC has received increasing attention because new catalysts, receptors, and sensors have been identified by using this approach.[2f–j]

The large advantage of DCC over CC is the template effect.[4,8] When a guest molecule is added to the dynamic combinatorial library (DCL), some of the building blocks present in the library bind to it more strongly, thus they will be removed from the pool of building blocks. Under appropriate experimental conditions,[9] the thermodynamic equilibrium of the library will shift to amplify good receptors. One example of receptor selection was described by Sanders and co-workers who showed the amplification of a receptor from a DCL of peptide hydrazones by metal ions.[10]

Despite the abundance of hydrogen bonds in nature, their use in the preparation of a DCL has not attracted much attention to date; this is probably because it is not easy to find a system that is self-assembled by using hydrogen bonds and is also able to recognize molecular guests by means of noncovalent interactions. Nevertheless, hydrogen bonds have the advantage of directionality, high selectivity, and comparable strength to one another. This comparable strength will lead to DCLs that exhibit an almost statistical distribution of library members.

To the best of our knowledge, all the DCLs described to date are based on receptors of different sizes (variable stoi-

[a] Dr. J. M. C. A. Kerckhoffs, Dr. M. A. Mateos-Timoneda, Prof. D. N. Reinhoudt, Dr. M. Crego-Calama
Laboratory of Supramolecular Chemistry and Technology
MESA+ Institute for Nanotechnology, University of Twente
P.O. Box 217, 7500 AE Enschede (The Netherlands)
Fax: (+31) 53-489-4645
E-mail: d.n.reinhoudt@tnw.utwente.nl
m.cregocalama@tnw.utwente.nl

Supporting information for this article is available on the WWW under http://www.chemeurj.org/ or from the author.

chiometry) with one[10,11] or more structurally diverse building blocks.[12] Aside from our own DCL,[13] there have been only two other examples of DCLs formed by assemblies with uniform stoichiometry.[14] However, these libraries have strong thermodynamic differentiation between DCL members as a result of steric and electronic effects.[9c]

In this paper, we describe the templating ability of a guest (noncovalent trimer $\mathbf{2a}_3$) in small DCLs of hydrogen-bonded *endo* receptors with uniform stoichiometry (double-rosette core). Furthermore, we show that amplified receptor $\mathbf{1a}_3$·$(DEB)_6$, formed by the self-assembly of six 5,5-diethyl barbiturate (DEB) molecules and three calix[4]arene dimelamine derivative **1a** molecules, is able to template the formation of the best-fitting guest trimer ($\mathbf{2a}_3$) from a library of structurally related guest molecules (Figure 1).

Results and Discussion

The self-assembled *endo* receptors $(\mathbf{1a–d})_3$·$(DEB)_6$ based on the double-rosette motif are formed upon mixing calix[4]arene dimelamines **1a–d** and DEB in a 1:2 ratio in [D_8]toluene.[15,16] These assemblies are held together by the formation of 36 cooperative hydrogen bonds. The top and bottom of these molecular boxes comprise cyclic hydrogen-bonded rosette motifs, with the calix[4]arene units acting as side walls. Structural diversity in these calix[4]arene double-rosette assemblies is generated simply by mixing the appropriate number of **1*x*** components (***x*** = **a**, **b**, …***N***) under thermodynamically controlled conditions.[7] As these hydrogen-bonded assemblies are kinetically labile, there is a continuous exchange of **1*x*** components between the different assemblies present. In this way, *M* heteromeric assemblies are formed in addition to *L* homomeric assemblies. The total number of assemblies (*P*) (i.e., *L*+*M*) present in such a library rapidly increases with an increasing number of components *N* and is given by Equation (1).

$$P = N^2 + \frac{N(N-1)(N-2)}{6} \quad (1)$$

DCLs from *endo* receptors $(\mathbf{1a–d})_3$·$(DEB)_6$: Previously, we have shown that receptor $\mathbf{1a}_3$·$(DEB)_6$ templates the regioselective formation of trimer $\mathbf{2a}_3$ within the receptor cavity (*endo* complexation).[17] Addition of three equivalents of alizarin **2a** to the self-assembled host $\mathbf{1a}_3$·$(DEB)_6$, which exhibits D_3 symmetry (staggered orientation of the two melamine rings of the calix[4]arene moieties), yielded the quantitative self-assembly of complex $\mathbf{1a}_3$·$(DEB)_6$·$\mathbf{2a}_3$ with C_{3h} symmetry (eclipsed orientation of the two melamine rings of the calix[4]arene moieties) in which encapsulated trimer $\mathbf{2a}_3$ is itself self-assembled by hydrogen bonds.

In this paper, we report the potential amplification of the best *endo* receptor $\mathbf{1}x_3$·$(DEB)_6$ (***x*** = **a–d**) by guest molecule **2a** in different libraries formed by the assemblies $(\mathbf{1a–d})_3$·$(DEB)_6$.[18]

First, we studied two different DCLs, $\mathbf{1a}_n$·$\mathbf{1b}_{(3-n)}$·$(DEB)_6$ (n = 0–3) and $\mathbf{1a}_n$·$\mathbf{1c}_{(3-n)}$·$(DEB)_6$ (n = 0–3), which were obtained by mixing structurally different calix[4]arene dimelamines **1a**+**1b** and **1a**+**1c**, respectively, with DEB in [D_8]toluene.[19]

Amplification studies

Four-component library $\mathbf{1a}_n$·$\mathbf{1b}_{(3-n)}$·$(DEB)_6$ *(*n*=0–3)*: Mixing double rosettes $\mathbf{1a}_3$·$(DEB)_6$ and $\mathbf{1b}_3$·$(DEB)_6$ (ratio 1:1) yields a mixture of homomeric and heteromeric assemblies $\mathbf{1a}_2$·$\mathbf{1b}_1$·$(DEB)_6$ and $\mathbf{1a}_1$·$\mathbf{1b}_2$·$(DEB)_6$ as a result of the

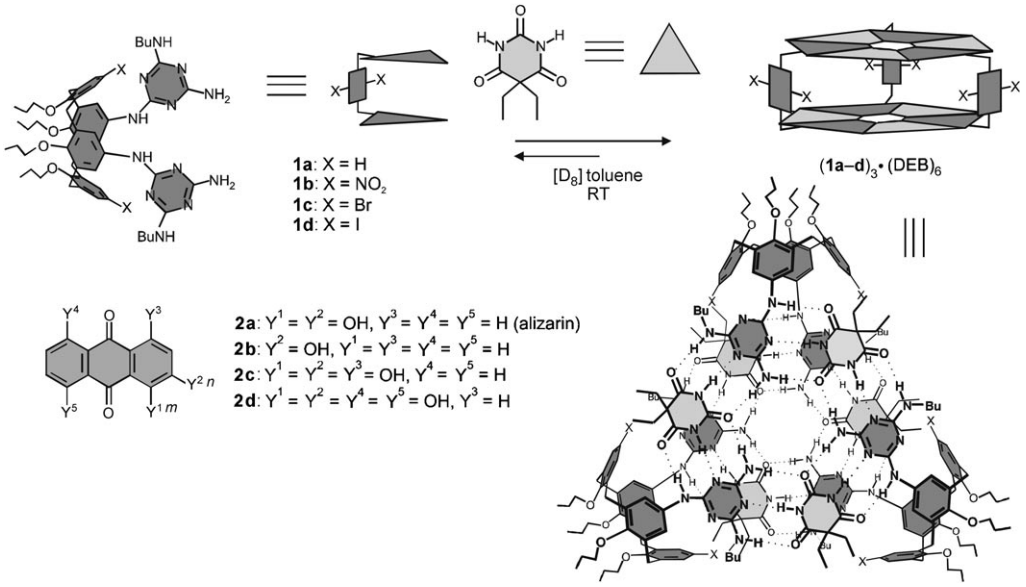

Figure 1. Molecular structures and schematic representations of compounds **1a–1d** and assembly formations $(\mathbf{1a–1d})_3$·$(DEB)_6$, and molecular structures of compounds **2a–d**.

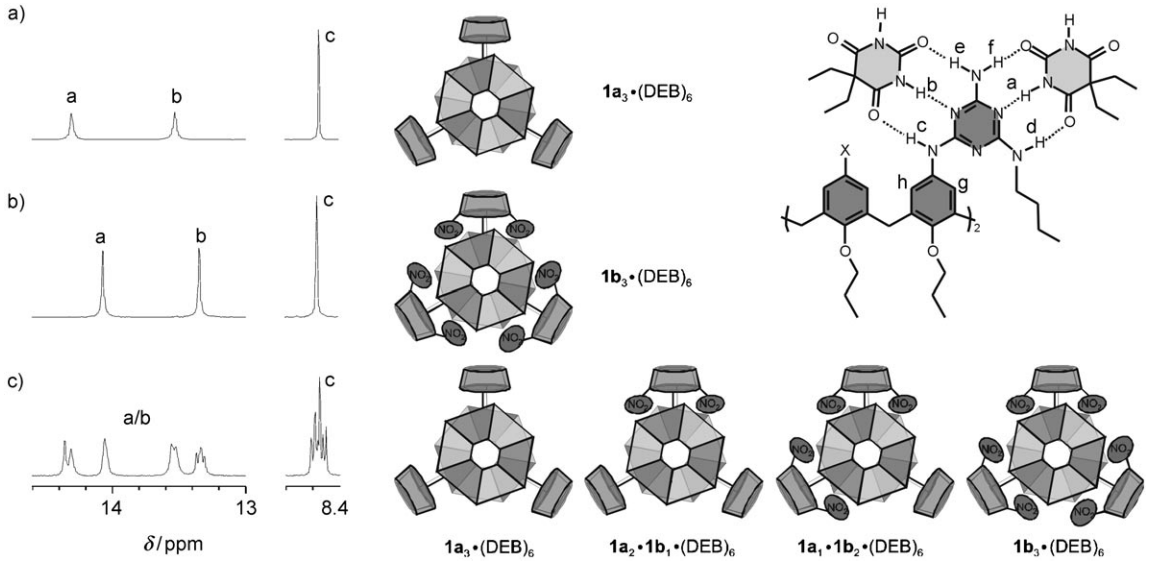

Figure 2. ^{1}H NMR spectra of a) assembly $\mathbf{1a}_3$·(DEB)$_6$, b) assembly $\mathbf{1b}_3$·(DEB)$_6$, and c) the dynamic mixture $\mathbf{1a}_n$·$\mathbf{1b}_{(3-n)}$·(DEB)$_6$ (n = 0–3). The spectra were recorded at 400 MHz at 298 K in [D$_8$]toluene.

continuous exchange of the individual components in [D$_8$]toluene.[7] ^{1}H NMR spectra (protons H^a, H^b, and H^c in Figure 2) clearly show this mixing process because heteromeric assemblies give rise to different signals for hydrogen-bonded protons. Furthermore, the ^{1}H NMR spectrum of the mixture (Figure 2c) shows that calix[4]arene dimelamines **1a** and **1b** are statistically distributed over the four assemblies in a ratio of 1:3:3:1 for $\mathbf{1a}_3$·(DEB)$_6$, $\mathbf{1a}_2$·$\mathbf{1b}_1$·(DEB)$_6$, $\mathbf{1a}_1$·$\mathbf{1b}_2$·(DEB)$_6$, and $\mathbf{1b}_3$·(DEB)$_6$, respectively.[7]

Upon addition of guest **2a** (1.2 equiv) to the dynamic mixture $\mathbf{1a}_n$·$\mathbf{1b}_{(3-n)}$·(DEB)$_6$ (n = 0–3) in [D$_8$]toluene (Figure 3), several signals in the ^{1}H NMR spectrum of the library shifted and new signals corresponding to the encapsulated guest appeared (Figure 4). The new OH^n signal at δ = 10.00 ppm corresponds to complex $\mathbf{1a}_3$·(DEB)$_6$·$\mathbf{2a}_3$ (Figure 4c; for the complete spectrum of $\mathbf{1a}_3$·(DEB)$_6$·$\mathbf{2a}_3$ and individual encapsulation studies of **2a** with $\mathbf{1a}_3$·(DEB)$_6$ or $\mathbf{1b}_3$·(DEB)$_6$, see the Supporting Information).[17] The presence of only one

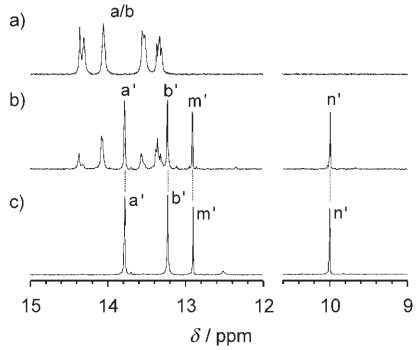

Figure 4. ^{1}H NMR spectra of dynamic mixture $\mathbf{1a}_n$·$\mathbf{1b}_{(3-n)}$·(DEB)$_6$ (n = 0–3) in a) the absence and b) the presence of **2a** (1.2 equiv), and c) of complex $\mathbf{1a}_3$·(DEB)$_6$·$\mathbf{2a}_3$. The spectra were recorded at 400 MHz at 298 K in [D$_8$]toluene.

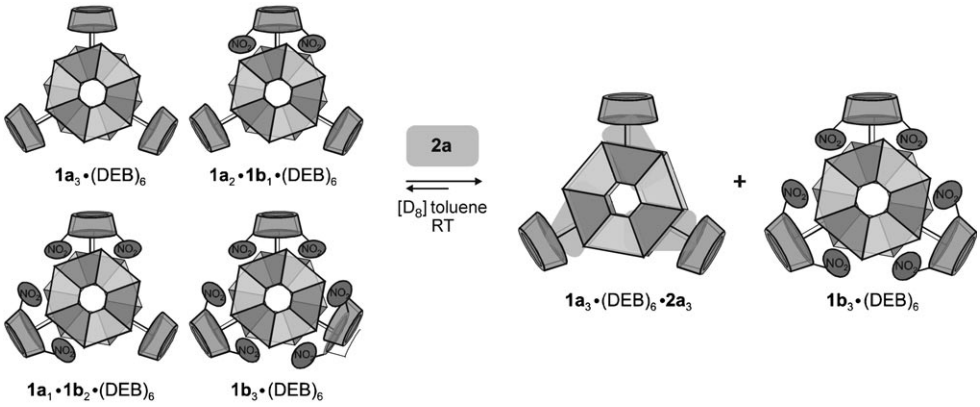

Figure 3. Schematic representation of the complete amplification of receptor $\mathbf{1a}_3$·(DEB)$_6$·$\mathbf{2a}_3$ upon addition of guest molecule **2a** from DCL $\mathbf{1a}_n$·$\mathbf{1b}_{(3-n)}$·(DEB)$_6$ (n = 0–3).

signal in this region indicates that only one complex is formed (Figure 4b). No other resonances are evident between $\delta = 9.0$–10.5 ppm that would correspond to a complex of $\mathbf{2a}_3$ with either $\mathbf{1b}_3{\cdot}(\mathrm{DEB})_6$ or the two heteromeric assemblies $\mathbf{1a}_n{\cdot}\mathbf{1b}_{(3-n)}{\cdot}(\mathrm{DEB})_6$ ($n = 1, 2$). The NH_{DEB} protons, H^a and H^b, show the amplification of receptor $\mathbf{1a}_3{\cdot}(\mathrm{DEB})_6$ in the mixture). Integration of NH_{DEB} protons H_a and H_b showed that complex $\mathbf{1a}_3{\cdot}(\mathrm{DEB})_6{\cdot}\mathbf{2a}_3$ represents approximately 35% of all assemblies present. The best binder $\mathbf{1a}_3{\cdot}(\mathrm{DEB})_6$ is enriched by a factor of 2.8 in the mixture (from $\approx 12.5\%$ initially to $\approx 35\%$ after addition of **2a**).

We wanted to verify that free assembly $\mathbf{1a}_3{\cdot}(\mathrm{DEB})_6$ was not present in the mixture, thus the signal for proton H^c was monitored (Figure 5). This proton resonates at $\delta = 8.55$ ppm

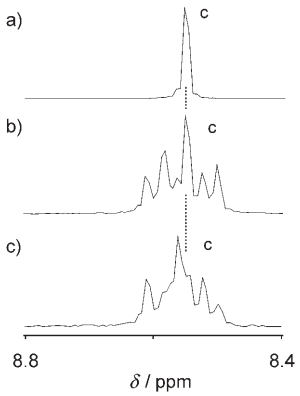

Figure 5. Part of the ^{1}H NMR spectra of a) assembly $\mathbf{1a}_3{\cdot}(\mathrm{DEB})_6$ and dynamic mixture $\mathbf{1a}_n{\cdot}\mathbf{1b}_{(3-n)}{\cdot}(\mathrm{DEB})_6$ ($n = 0$–3) in b) the absence and c) the presence of **2a** (1.2 equiv). The spectra were recorded at 400 MHz at 298 K in [D_8]toluene.

in the free assembly (Figure 5a) (H^c resonates at $\delta = 8.16$ ppm in complex $\mathbf{1a}_3{\cdot}(\mathrm{DEB})_6{\cdot}\mathbf{2a}_3$). Therefore, the disappearance of the resonance at $\delta = 8.55$ ppm would prove that there is no free assembly $\mathbf{1a}_3{\cdot}(\mathrm{DEB})_6$ present in solution. Unfortunately, this signal overlaps with the resonance for H^c in $\mathbf{1a}_1{\cdot}\mathbf{1b}_2{\cdot}(\mathrm{DEB})_6$.[7] However, integration of the different proton signals for H^c indicated that free assembly $\mathbf{1a}_3{\cdot}(\mathrm{DEB})_6$ was not present in solution in significant quantities.

Four-component library $\boldsymbol{1a_n{\cdot}1c_{(3-n)}{\cdot}(DEB)_6}$ *(*$n = 0$–*3)*: DCL $\mathbf{1a}_n{\cdot}\mathbf{1c}_{(3-n)}{\cdot}(\mathrm{DEB})_6$ ($n = 0$–3) was prepared by mixing equimolar solutions of individual double rosettes $\mathbf{1a}_3{\cdot}(\mathrm{DEB})_6$ and $\mathbf{1c}_3{\cdot}(\mathrm{DEB})_6$ in [D_8]toluene at room temperature. The formation of heteromeric assemblies $\mathbf{1a}_n{\cdot}\mathbf{1c}_{(3-n)}{\cdot}(\mathrm{DEB})_6$ ($n = 1, 2$) could be concluded from the multiple signals (at least 7) observed for H^c ($\delta = 8.67$–8.50 ppm) in the ^{1}H NMR spectrum (Figure 6c). This proton resonates as a singlet at $\delta = 8.55$ and 8.60 ppm for both homomeric assemblies $\mathbf{1a}_3{\cdot}(\mathrm{DEB})_6$ and $\mathbf{1c}_3{\cdot}(\mathrm{DEB})_6$, respectively (Figures 6a and b). Similar multiple resonances for other protons in the rosette were observed. Integration of the signals observed for H^c indicated an approximately statistical composition of the

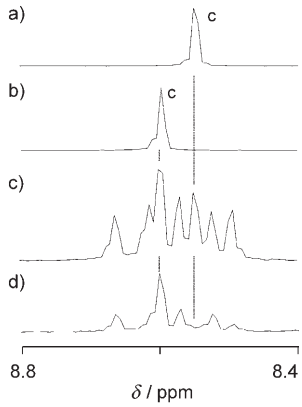

Figure 6. Part of the ^{1}H NMR spectra of assemblies a) $\mathbf{1a}_3{\cdot}(\mathrm{DEB})_6$ and b) $\mathbf{1c}_3{\cdot}(\mathrm{DEB})_6$, and dynamic mixture $\mathbf{1a}_n{\cdot}\mathbf{1c}_{(3-n)}{\cdot}(\mathrm{DEB})_6$ ($n = 0$–3) in c) the absence and d) the presence of **2a** (2 equiv). The spectra were recorded at 400 MHz at 298 K in [D_8]toluene.

mixture $(\mathbf{1a}_3{\cdot}(\mathrm{DEB})_6/\mathbf{1a}_2{\cdot}\mathbf{1c}_1{\cdot}(\mathrm{DEB})_6/\mathbf{1a}_1{\cdot}\mathbf{1c}_2{\cdot}(\mathrm{DEB})_6)/\mathbf{1c}_3{\cdot}(\mathrm{DEB})_6$ 1:3:3:1).

Addition of **2a** (2 equiv) to dynamic mixture $\mathbf{1a}_n{\cdot}\mathbf{1c}_{(3-n)}{\cdot}(\mathrm{DEB})_6$ ($n = 0$–3) shifted the equilibrium towards the most strongly binding assembly ($\mathbf{1a}_3{\cdot}(\mathrm{DEB})_6$). Integration of the signals in the ^{1}H NMR spectrum for rosette NH_{DEB} protons H^a and H^b, and the OH^m and OH^n protons of guest **2a** showed that approximately 48% of the assemblies encapsulated **2a**.[20] Integration of the OH^n signals showed that approximately 43% of these complexes (by regarding 48% total complex formation as 100%) correspond to homomeric complex $\mathbf{1a}_3{\cdot}(\mathrm{DEB})_6{\cdot}\mathbf{2a}_3$. Heteromeric complex $\mathbf{1a}_2{\cdot}\mathbf{1c}_1{\cdot}(\mathrm{DEB})_6{\cdot}\mathbf{2a}_3$ is formed in approximately 47% yield and complex $\mathbf{1a}_1{\cdot}\mathbf{1c}_2{\cdot}(\mathrm{DEB})_6{\cdot}\mathbf{2a}_3$ in approximately 10% yield, whereas the formation of homomeric complex $\mathbf{1c}_3{\cdot}(\mathrm{DEB})_6{\cdot}\mathbf{2a}_3$ is negligible. In dynamic mixture $\mathbf{1a}_n{\cdot}\mathbf{1c}_{(3-n)}{\cdot}(\mathrm{DEB})_6$ ($n = 0$–3), assembly $\mathbf{1a}_3{\cdot}(\mathrm{DEB})_6$ is present in approximately 13% yield before the addition of **2a**, whereas after addition of **2a**, complex $\mathbf{1a}_3{\cdot}(\mathrm{DEB})_6{\cdot}\mathbf{2a}_3$ is present in approximately 21% yield. Figure 7c shows that the resonance for proton H^c of homomeric assembly $\mathbf{1a}_3{\cdot}(\mathrm{DEB})_6$ completely disappears, which means that no free assembly $\mathbf{1a}_3{\cdot}(\mathrm{DEB})_6$ is present in solution. Thus, $\mathbf{1a}_3{\cdot}(\mathrm{DEB})_6$ is amplified by a factor of 1.6 in the DCL. The observed enrichment of $\mathbf{1a}_3{\cdot}(\mathrm{DEB})_6$ in DCL $\mathbf{1a}_n{\cdot}\mathbf{1c}_{(3-n)}{\cdot}(\mathrm{DEB})_6$ ($n = 0$–3) is smaller than the enrichment in DCL $\mathbf{1a}_n{\cdot}\mathbf{1b}_{(3-n)}{\cdot}(\mathrm{DEB})_6$ ($n = 0$–3), which probably indicates that the difference in binding affinity between **1a** and **1c** is smaller than that between **1a** and **1b**. Similar results were obtained for DCL $\mathbf{1a}_n{\cdot}\mathbf{1d}_{(3-n)}{\cdot}(\mathrm{DEB})_6$ ($n = 0$–3).[21]

To verify the difference in binding affinity, the encapsulation of **2a** by assemblies $\mathbf{1c}_3{\cdot}(\mathrm{DEB})_6$ or $\mathbf{1d}_3{\cdot}(\mathrm{DEB})_6$, which contain bromo and iodo substituents on the calix[4]arene moiety, respectively (Figure 1), were studied individually (for details of the individual encapsulation studies of **2a** with $\mathbf{1c}_3{\cdot}(\mathrm{DEB})_6$, see the Supporting Information). In contrast to results obtained for $\mathbf{1a}_3{\cdot}(\mathrm{DEB})_6$ and $\mathbf{1b}_3{\cdot}(\mathrm{DEB})_6$ (see the Supporting Information), upon addition of **2a** (3.2 equiv for $\mathbf{1c}_3{\cdot}(\mathrm{DEB})_6$ and 2.7 equiv for $\mathbf{1d}_3{\cdot}(\mathrm{DEB})_6$),

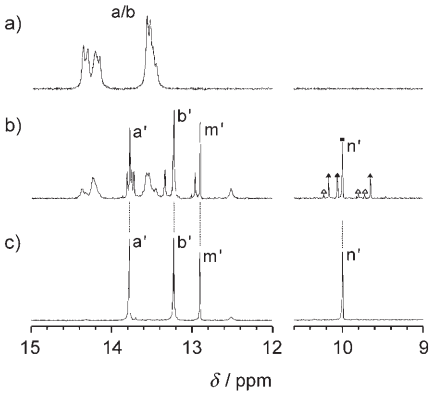

Figure 7. Part of the ^{1}H NMR spectra of dynamic mixture $\mathbf{1a}_n$·$\mathbf{1c}_{(3-n)}$·$(DEB)_6$ (n=0–3) in a) the absence and b) the presence of **2a** (2 equiv), and c) of complex $\mathbf{1a}_3$·$(DEB)_6$·$\mathbf{2a}_3$. The spectra were recorded at 400 MHz at 298 K in [D_8]toluene. ■ represents complex $\mathbf{1a}_3$·$(DEB)_6$·$\mathbf{2a}_3$, ▲ represents complex $\mathbf{1a}_2$·$\mathbf{1c}_1$·$(DEB)_6$·$\mathbf{2a}_3$, and △ represents complex $\mathbf{1a}_1$·$\mathbf{1c}_2$·$(DEB)_6$·$\mathbf{2a}_3$.

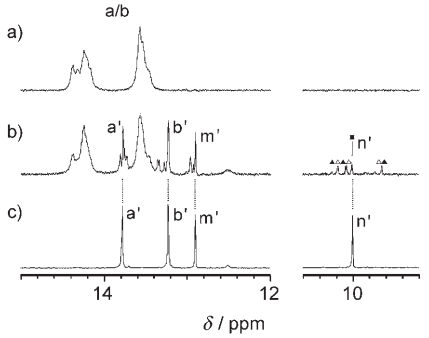

Figure 8. Part of the ^{1}H NMR spectra of dynamic mixture $\mathbf{1a}_n$·$\mathbf{1c}_m$·$\mathbf{1d}_{(3-(n+m))}$·$(DEB)_6$ (n=0–3; m=0–3; $(n+m)\leq 3$) in a) the absence and b) the presence of **2a** (2 equiv), and c) of complex $\mathbf{1a}_3$·$(DEB)_6$·$\mathbf{2a}_3$. The spectra were recorded at 400 MHz at 298 K in [D_8]toluene. ■ represents complex $\mathbf{1a}_3$·$(DEB)_6$·$\mathbf{2a}_3$, ▲ represents complex $\mathbf{1a}_2$·$\mathbf{1d}_1$·$(DEB)_6$·$\mathbf{2a}_3$, and △ represents complex $\mathbf{1a}_2$·$\mathbf{1c}_1$·$(DEB)_6$·$\mathbf{2a}_3$.

two new, different sets of signals (instead of one) appeared in the ^{1}H NMR spectrum for each assembly (2 mM in [D_8]toluene). Each set of signals corresponds to two different 3:1 $\mathbf{1c}_3$·$(DEB)_6$·$\mathbf{2a}_3$ complexes (complex-1 and complex-2, see the Supporting Information). Furthermore, the free assembly was observed in both instances, which was not the case for receptors $\mathbf{1a}_3$·$(DEB)_6$ and $\mathbf{1b}_3$·$(DEB)_6$. As revealed by the intensities of the resonances in the ^{1}H NMR spectrum for assembly $\mathbf{1c}_3$·$(DEB)_6$, 38% of complex-1, 12% of complex-2, and 50% of the free assembly were observed after addition of **2a** (see the Supporting Information), which explains the smaller amplification factor observed for this library.

For assembly $\mathbf{1d}_3$·$(DEB)_6$, 37% of complex-1, 22% of complex-2, and 49% of the free assembly $\mathbf{1d}_3$·$(DEB)_6$ was present in the library after addition of **2a** (2.7 equiv).

Ten-component library $\mathbf{1a}_n$·$\mathbf{1c}_m$·$\mathbf{1d}_{(3-(n+m))}$·*(DEB)$_6$* (n=*0–3;* m=*0–3;* (n+m)$\leq$*3)*: Subsequently, the behavior of a ten-component DCL was investigated. Dynamic mixture $\mathbf{1a}_n$·$\mathbf{1c}_m$·$\mathbf{1d}_{(3-(n+m))}$·$(DEB)_6$ (n=0–3; m=0–3; $(n+m)\leq 3$) was prepared by mixing equimolar solutions of individual double rosettes $\mathbf{1a}_3$·$(DEB)_6$, $\mathbf{1c}_3$·$(DEB)_6$, and $\mathbf{1d}_3$·$(DEB)_6$ in [D_8]toluene at room temperature. The ^{1}H NMR spectrum becomes too complex for the calculation of the distribution of **1a**, **1c**, and **1d** over the different assemblies (Figure 8a). However, after the addition of **2a** (0.7 equiv), the OH^n resonances indicate the different complexes that have been formed (Figure 8b). The total complex formation is around 20%. Homomeric complex $\mathbf{1a}_3$·$(DEB)_6$·$\mathbf{2a}_3$ (■ in Figure 8b) is present in approximately 39% yield, whereas the two heteromeric complexes $\mathbf{1a}_2$·$\mathbf{1c}_1$·$(DEB)_6$·$\mathbf{2a}_3$ (△ in Figure 8b) and $\mathbf{1a}_2$·$\mathbf{1d}_1$·$(DEB)_6$·$\mathbf{2a}_3$ (▲ in Figure 8b) are both present in around 28% yield of the total complexes. If the distribution of **1a**, **1c**, and **1d** over the assemblies were statistical, then assembly $\mathbf{1a}_3$·$(DEB)_6$ would only be present in 3.7% yield (Table 1). Complex $\mathbf{1a}_3$·$(DEB)_6$·$\mathbf{2a}_3$ is present in approximately 7.8% yield after addition of **2a**, which is an enrichment factor of around 2.

Table 1. The statistical composition of the ten-component library.[a]

Assemblies	Statistical distribution[b] fraction	[%]
$\mathbf{1a}_3$·$(DEB)_6$, $\mathbf{1c}_3$·$(DEB)_6$, $\mathbf{1d}_3$·$(DEB)_6$	1/27	3.70
$\mathbf{1a}_2$·$\mathbf{1c}_1$·$(DEB)_6$, $\mathbf{1a}_1$·$\mathbf{1c}_2$·$(DEB)_6$, $\mathbf{1a}_2$·$\mathbf{1d}_1$·$(DEB)_6$, $\mathbf{1a}_1$·$\mathbf{1d}_2$·$(DEB)_6$, $\mathbf{1c}_2$·$\mathbf{1d}_1$·$(DEB)_6$, $\mathbf{1c}_1$·$\mathbf{1d}_2$·$(DEB)_6$	3/27	11.11
$\mathbf{1a}_1$·$\mathbf{1c}_1$·$\mathbf{1d}_1$·$(DEB)_6$	6/27	22.22

[a] The different components are mixed in equimolar amounts. [b] Of each assembly.

Twenty-component library $\mathbf{1a}_n$·$\mathbf{1b}_m$·$\mathbf{1c}_o$·$\mathbf{1d}_{(3-(n+m+o))}$·*(DEB)$_6$* (n=*0–3;* m=*0–3;* o=*0–3;* (n+m+o)$\leq$*3)*: Finally, amplification in a twenty-component DCL templated by trimer $\mathbf{2a}_3$ was investigated. Statistically, assembly $\mathbf{1a}_3$·$(DEB)_6$ would only account for 1.56% (Table 2) of the assemblies in dy-

Table 2. The statistical composition of the twenty-component library.[a]

Assemblies	Statistical distribution[b] fraction	[%]
$\mathbf{1a}_3$·$(DEB)_6$, $\mathbf{1b}_3$·$(DEB)_6$, $\mathbf{1c}_3$·$(DEB)_6$, $\mathbf{1d}_3$·$(DEB)_6$	1/64	1.56
$\mathbf{1a}_2$·$\mathbf{1b}_1$·$(DEB)_6$, $\mathbf{1a}_1$·$\mathbf{1b}_2$·$(DEB)_6$, $\mathbf{1a}_2$·$\mathbf{1c}_1$·$(DEB)_6$, $\mathbf{1a}_1$·$\mathbf{1c}_2$·$(DEB)_6$, $\mathbf{1a}_2$·$\mathbf{1d}_1$·$(DEB)_6$, $\mathbf{1a}_1$·$\mathbf{1d}_2$·$(DEB)_6$, $\mathbf{1b}_2$·$\mathbf{1c}_1$·$(DEB)_6$, $\mathbf{1b}_1$·$\mathbf{1c}_2$·$(DEB)_6$, $\mathbf{1b}_2$·$\mathbf{1d}_1$·$(DEB)_6$, $\mathbf{1b}_1$·$\mathbf{1d}_2$·$(DEB)_6$, $\mathbf{1c}_2$·$\mathbf{1d}_1$·$(DEB)_6$, $\mathbf{1c}_1$·$\mathbf{1d}_2$·$(DEB)_6$	3/64	4.69
$\mathbf{1a}_1$·$\mathbf{1b}_1$·$\mathbf{1c}_1$·$(DEB)_6$, $\mathbf{1a}_1$·$\mathbf{1b}_1$·$\mathbf{1d}_1$·$(DEB)_6$, $\mathbf{1a}_1$·$\mathbf{1c}_1$·$\mathbf{1d}_1$·$(DEB)_6$, $\mathbf{1b}_1$·$\mathbf{1c}_1$·$\mathbf{1d}_1$·$(DEB)_6$	6/64	9.37

[a] The different components are mixed in equimolar amounts. [b] Of each assembly.

namic mixture $\mathbf{1a}_n\cdot\mathbf{1b}_m\cdot\mathbf{1c}_o\cdot\mathbf{1d}_{(3-(n+m+o))}\cdot(\mathrm{DEB})_6$ (n, m, $o=0$–3; $(n+m+o)\leq 3$) because the individual assemblies are mixed in equal amounts (Figure 9a). After addition of **2a**

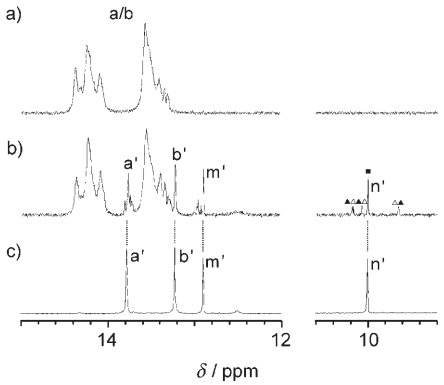

Figure 9. ^{1}H NMR spectra of dynamic mixture $\mathbf{1a}_n\cdot\mathbf{1b}_m\cdot\mathbf{1c}_o\cdot\mathbf{1d}_{(3-(n+m+o))}\cdot(\mathrm{DEB})_6$ ($n=0$–3; $m=0$–3; $o=1$–3; $(n+m+o)\leq 3$) in a) the absence and b) the presence of **2a** (2 equiv), and c) of complex $\mathbf{1a}_3\cdot(\mathrm{DEB})_6\cdot\mathbf{2a}_3$. The spectra were recorded at 400 MHz at 298 K in [D$_8$]toluene. ■ represents complex $\mathbf{1a}_3\cdot(\mathrm{DEB})_6\cdot\mathbf{2a}_3$, ▲ represents complex $\mathbf{1a}_2\cdot\mathbf{1d}_1\cdot(\mathrm{DEB})_6\cdot\mathbf{2a}_3$, and △ represents complex $\mathbf{1a}_2\cdot\mathbf{1c}_1\cdot(\mathrm{DEB})_6\cdot\mathbf{2a}_3$.

(0.5 equiv) to the dynamic mixture, the resonances for OH^n indicate which complexes are formed. In total, approximately 10% of all assemblies encapsulated the $\mathbf{2a}_3$ trimer. Homomeric complex $\mathbf{1a}_3\cdot(\mathrm{DEB})_6\cdot\mathbf{2a}_3$ (■ in Figure 9b) is present in approximately 49% yield and the two heteromeric complexes, $\mathbf{1a}_2\cdot\mathbf{1c}_1\cdot(\mathrm{DEB})_6\cdot\mathbf{2a}_3$ (△ in Figure 9b) and $\mathbf{1a}_2\cdot\mathbf{1d}_1\cdot(\mathrm{DEB})_6\cdot\mathbf{2a}_3$ (▲ in Figure 9b), are both present in around 25% yield of the total amount of the complexes. Thus, complex $\mathbf{1a}_3\cdot(\mathrm{DEB})_6\cdot\mathbf{2a}_3$ is present in approximately 4.7% yield in the dynamic mixture after the addition of **2a**, which shows an enrichment factor of about 2.8. Thus, trimer $\mathbf{2a}_3$ is even capable of selecting the most strongly binding assembly ($\mathbf{1a}_3\cdot(\mathrm{DEB})_6$) from a twenty-component library.

Template effect of the *endo* receptor 1a·(DEB)$_6$ in a library of guest molecules 2a–d: We changed the role of receptor and guest to study the potential for receptor $\mathbf{1a}_3\cdot(\mathrm{DEB})_6$ to act as a template for the formation and selection of the best-fitting trimer guest from a mixture of guest molecules **2a–d** (Figure 1).

First, a mixture of only two guest molecules **2a** and **2b** with receptor $\mathbf{1a}_3\cdot(\mathrm{DEB})_6$ was studied. The library was obtained by mixing a 1:1 ratio of a solution of complex $\mathbf{1a}_3\cdot(\mathrm{DEB})_6$ (1 mM in $CDCl_3$) and **2a** (4 equiv) with a solution of $\mathbf{1a}_3\cdot(\mathrm{DEB})_6$ (1 mM in $CDCl_3$) and **2b** (3.8 equiv).[22] The ^{1}H NMR spectrum of the mixture showed additional signals compared with the ^{1}H NMR spectra of the two individual complexes (Figure 10), which revealed the formation of heteromeric (related to the guest molecules) complexes $\mathbf{1a}_3\cdot(\mathrm{DEB})_6\cdot\mathbf{2a}_n\cdot\mathbf{2b}_{(3-n)}$ ($n=1$, 2). The hydroxyl group OH^m, only present in **2a**, gave four different signals in the ^{1}H NMR spectrum of the library (Figure 10c). One of the signals clearly comes from homomeric complex $\mathbf{1a}_3\cdot(\mathrm{DEB})_6\cdot\mathbf{2a}_3$. The other three signals arise from the two heteromeric complexes, that is, one signal for complex $\mathbf{1a}_3\cdot(\mathrm{DEB})_6\cdot\mathbf{2a}_1\cdot\mathbf{2b}_2$ and two broader signals for $\mathbf{1a}_3\cdot(\mathrm{DEB})_6\cdot\mathbf{2a}_2\cdot\mathbf{2b}_1$. The intensities of all four signals are comparable. The signal derived from homomeric complex $\mathbf{1a}_3\cdot(\mathrm{DEB})_6\cdot\mathbf{2a}_3$ accounts for three **2a** molecules, and therefore its abundance is three times smaller than the heteromeric complex. Integration of the signals indicates that the relative concentrations of the four different complexes, $\mathbf{1a}_3\cdot(\mathrm{DEB})_6\cdot\mathbf{2a}_n\cdot\mathbf{2b}_{(3-n)}$ ($n=0$–3), in the mixture is 1:3:3:1 ($\mathbf{2a}_3/\mathbf{2a}_2\cdot\mathbf{2b}/\mathbf{2a}\cdot\mathbf{2b}_2/\mathbf{2b}_3$), in agreement with the statistical distribution of guest molecules **2a** and **2b** over the various assemblies.[23] Thus, there is no preference for the encapsulation of exclusively **2a** or **2b**, which indicates a similar binding affinity for both molecules to receptor $\mathbf{1a}_3\cdot(\mathrm{DEB})_6$. The OH^n proton was expected to result in eight different signals, one for each homomeric complex and three for each heteromeric complex. The expected signals partially overlap with each other, which results in a set of

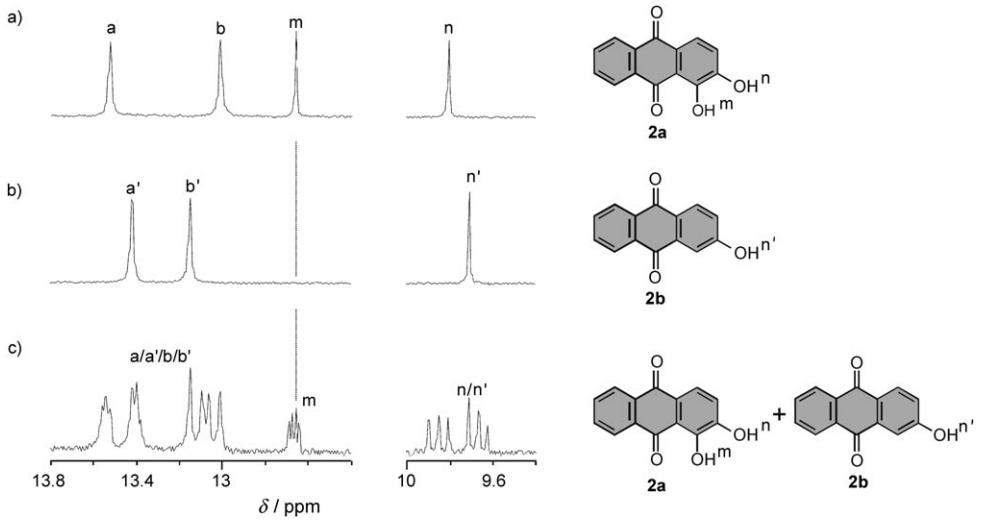

Figure 10. Part of the ^{1}H NMR spectrum for the complexation of $\mathbf{1a}_3\cdot(\mathrm{DEB})_6$ and a) **2a**, b) **2b**, and c) 1:1 mixture of **2a** and **2b**.

signals that is difficult to analyze. For the NH_{DEB} protons H_a and H_b, around ten different signals were observed.

Owing to the complexity of the ^{1}H NMR spectra, matrix-assisted laser desorption ionization time-of-flight (MALDI-TOF) mass spectrometry experiments using Ag^+ to ionize the double-rosette assemblies were also used to characterize the different double-rosette complexes.[24,25] The MALDI-TOF spectrum of a sample containing complex $\mathbf{1a}_3$·$(DEB)_6$·$\mathbf{2a}_3$ showed an intense signal corresponding to the 1:1 ($\mathbf{1a}_3$·$(DEB)_6$·$\mathbf{2a}$) complex and a smaller signal corresponding to the 1:2 ($\mathbf{1a}_3$·$(DEB)_6$·$\mathbf{2a}_2$) complex, whereas the signal for the 1:3 ($\mathbf{1a}_3$·$(DEB)_6$·$\mathbf{2a}_3$) complex was hardly observed. Also for the sample containing complex $\mathbf{1a}_3$·$(DEB)_6$·$\mathbf{2b}_3$ a similar signal distribution was found in the MALDI-TOF mass spectrum.

When the sample containing assembly $\mathbf{1a}_3$·$(DEB)_6$ (0.25 mM), **2a** (3.8 equiv), and **2b** (2.6 equiv) was measured by using MALDI-TOF mass spectrometry, only signals corresponding to the different combinations (homo- and heteromeric) of the 1:3 complexes ($\mathbf{1a}_3$·$(DEB)_6$·$\mathbf{2a}_n$·$\mathbf{2b}_{(3-n)}$ ($n=$ 0–3)) were observed in the *m*/*z* spectrum. No signals corresponding to 1:1 and 1:2 complexes were found. Two different signals corresponding to the two homomeric complexes were observed at *m*/*z* 4798 (calcd for $\mathbf{1a}_3$·$(DEB)_6$·$\mathbf{2a}_3$·Ag^+: 4799) and at *m*/*z* 4753 (calcd for $\mathbf{1a}_3$·$(DEB)_6$·$\mathbf{2b}_3$·Ag^+: 4751), and another two signals corresponding to the heteromeric complexes at *m*/*z* 4781 (calcd for $\mathbf{1a}_3$·$(DEB)_6$·$\mathbf{2a}_2$·$\mathbf{2b}_1$·Ag^+: 4783) and at *m*/*z* 4764 (calcd for $\mathbf{1a}_3$·$(DEB)_6$·$\mathbf{2a}_1$·$\mathbf{2b}_2$·Ag^+: 4767). The different behavior observed between the complexes with one assembly and only one type of guest molecule versus multiple guest molecules is still unclear.

A similar mixture of guest molecules **2a** and **2d** was also investigated with a 1:1 mixture of assembly $\mathbf{1a}_3$·$(DEB)_6$ (1 mM in $CDCl_3$) with **2a** (4 equiv), and of assembly $\mathbf{1a}_3$·$(DEB)_6$ (1 mM in $CDCl_3$) with **2d** (3.8 equiv[26]). The ^{1}H NMR spectrum of this mixture showed only signals for the encapsulation of trimer $\mathbf{2a}_3$ by assembly $\mathbf{1a}_3$·$(DEB)_6$, and no signals for either homomeric complex $\mathbf{1a}_3$·$(DEB)_6$·$\mathbf{2d}_3$ or the two heteromeric complexes $\mathbf{1a}_3$·$(DEB)_6$·$\mathbf{2a}_2$·$\mathbf{2d}_1$ and $\mathbf{1a}_3$·$(DEB)_6$·$\mathbf{2a}_1$·$\mathbf{2d}_2$ were observed (Figure 11). Thus, guest **2d** is not complexed by assembly $\mathbf{1a}_3$·$(DEB)_6$. Additionally, the signals for the free assembly are visible in the ^{1}H NMR spectrum as a consequence of the number of equivalents of **2a** (2 equiv) relative to the total amount of double rosette $\mathbf{1a}_3$·$(DEB)_6$ present. In conclusion, receptor $\mathbf{1a}_3$·$(DEB)_6$ is capable of selecting the best guest from a pool of two guest molecules. Furthermore, it is the first time that selective noncovalent synthesis by using a receptor in a virtual library of self-assembled guests has been achieved.

Unfortunately, the ^{1}H NMR and MALDI-TOF mass spectra for the sample that contained assembly $\mathbf{1a}_3$·$(DEB)_6$ and the four guest molecules **2a**–**2d** were too complicated to provide relevant information.

Conclusion

We have shown that small dynamic combinatorial libraries from calix[4]arene dimelamines **1a**–**d** and DEB are formed upon simply mixing the appropriate building blocks in the appropriate stoichiometry. Furthermore, we have shown that the selection of the best binder is achieved after guest addition. The largest amplification factor (2.8) was observed after addition of **2a** to the four-component library $\mathbf{1a}_n$·$\mathbf{1b}_{(3-n)}$·$(DEB)_6$ ($n=0$–3). Addition of **2a** to the twenty-component library of $\mathbf{1a}_n$·$\mathbf{1b}_m$·$\mathbf{1c}_o$·$\mathbf{1d}_{(3-(n+m+o))}$·$(DEB)_6$ (n, m, $o=0$–3; $(n+m+o)\leq 3$) also showed amplification of the best binder $\mathbf{1a}_3$·$(DEB)_6$.

In the second part of the paper we showed that the best receptor ($\mathbf{1a}_3$·$(DEB)_6$) allows the selective encapsulation of the best-fitting guest from a library of "virtual" self-assembled trimers. Unfortunately, the characterization of the libraries by using ^{1}H NMR spectroscopy becomes very complex as the libraries become larger. Also, MALDI-TOF mass spectrometry is not an appropriate technique because the distribution of the different assemblies in the spectra does not correspond to the abundance of the mixture in solution, probably because the assemblies have different ionization energies.

Overall, we have described how hydrogen-bonding motifs allow the formation of dynamic mixtures of both receptor and guest molecules. Both selection and amplification of the best guest or the best receptor is observed.

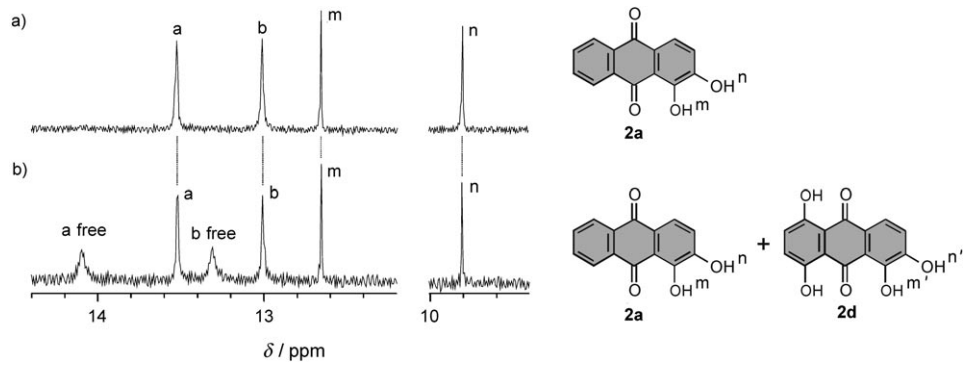

Figure 11. Part of the ^{1}H NMR spectrum for the complexation of a) **2a** to $\mathbf{1a}_3$·$(DEB)_6$ and b) a mixture of **2a** and **2d** to $\mathbf{1a}_3$·$(DEB)_6$.

Experimental Section

^{1}H NMR spectra were recorded at 400 MHz on a Varian Unity 400 WB spectrometer with either tetramethylsilane (TMS) or the solvent as an internal reference. The 2D double-quantum-filtered correlation spectroscopy (DQF-COSY) consisted of 2048 data points in t_2 and 267 increments in t_1. For the TOCSY experiment, the total

TOCSY mixing time was set to 65 ms. The spectrum was acquired with 2048 data points in t_2 and 267 free induction decays (FIDs) in t_1. The NOESY experiments were acquired with a mixing time of 90 ms, 2048 datapoints in t_2 and 267 increments in t_1. Mass spectrometry was performed by using a modified MALDI-TOF instrument (Voyager RP-DE, Perseptive Biosystems/Applied Biosystems, Framingham, MA, USA), equipped with delayed extraction and a $\lambda = 337$ nm UV nitrogen laser producing 2 ns pulses. Mass spectra were obtained in a linear mode. No organic acid matrix could be used during the experiments owing to the instability of the assemblies. A sample of known concentration (8–10 μL) was deposited on the (cold) spot well by adding 0.5 μL of a 10^{-6} molar solution of $AgOOCCF_3$. The samples were covered by a nonacidic liquid-polymer film that does not interact with the samples. To avoid crystallization of the samples, the pressure in the ion source was reduced drastically, which kept the pressure in the time-of-flight region under relatively high vacuum. The samples were introduced through a sample-plate insertion system at near-atmospheric pressure. Threshold laser energies were used to avoid fragmentation as a result of the high-energy laser power. After each experiment internal calibrations were performed by using a mixture of known proteins (ACTH 1-36, bovine insulin B oxidized, bovine insulin, myoglobin (horse heart) and cytochrome C (horse heart)) for the selected mass range.

Compounds **1a**–**1b**,[6] **1d**[6] and **1c**[27] were prepared according to methods previously described.

Formation of assemblies (1a–d)$_3$·(DEB)$_6$: Hydrogen-bonded assemblies (**1a**–**d**)$_3$·(DEB)$_6$ were prepared by mixing calix[4]arene dimelamines **1a**–**d** with DEB (2.5 equiv) in [D_8]toluene for 15 min.

Acknowledgements

This work is partially supported by the Technology Foundation of the Netherlands (J.M.C.A.K.).

[1] For examples of combinatorial libraries, see: a) K. B. Jensen, T. M. Braxmeier, M. Demarcus, J. G. Frey, J. D. Kilburn, *Chem. Eur. J.* **2002**, *8*, 1300–1309; b) R. Xu, G. Greiveldinger, L. E. Marenus, A. Cooper, J. A. Ellman, *J. Am. Chem. Soc.* **1999**, *121*, 4898–4899; c) H. S. Park, Q. Lin, A. D. Hamilton, *J. Am. Chem. Soc.* **1999**, *121*, 8–13.

[2] For recent reviews in the field of dynamic combinatorial chemistry, see: a) S. Otto, R. L. E. Furlan, J. K. M. Sanders, *Curr. Opin. Chem. Biol.* **2002**, *6*, 321–327; b) J.-M. Lehn, A. V. Eliseev, *Science* **2001**, *291*, 2331–2332; c) S. Otto, R. L. E. Furlan, J. K. M. Sanders, *Drug Discovery Today* **2002**, *7*, 117–125; d) O. Ramstrom, J.-M Lehn, *Nat. Rev. Drug Discovery* **2002**, *1*, 26–36; e) S. J. Rowan, S. J. Cantrill, G. R. L. Cousins, J. K. M. Sanders, J. F. Stoddart, *Angew. Chem.* **2002**, *114*, 938–993; *Angew. Chem. Int. Ed.* **2002**, *41*, 898–952; for examples of functional DCC, see: f) A. Buryak, K. Severin, *Angew. Chem.* **2005**, *117*, 8148–8152; *Angew. Chem. Int. Ed.* **2005**, *44*, 7935–7938; g) B. Brisig, J. K. M. Sanders, S. Otto. *Angew. Chem.* **2003**, *115*, 1308–1311; *Angew. Chem. Int. Ed.* **2003**, *42*, 1270–1273; h) T. Nishinaga, A. Tanatani, K. Oh, J. S. Moore, *J. Am. Chem. Soc.* **2002**, *124*, 5934–5935; i) T. S. R. Lam, A. Belenguer, S. L. Roberts, C. Naumann, T. Jarrosson, S. Otto, J. K. M. Sanders, *Science* **2005**, *308*, 667–669; j) S. Kubik, R. Goddard, S. Otto, S. Pohl, C. Reyheller, S. Stüwe, *Biosens. Bioelectron.* **2005**, *20*, 2364–2375.

[3] a) N. Sreenivasachary, J.-M. Lehn, *Proc. Natl. Acad. Sci. USA* **2005**, *102*, 5938–5943; b) E. Kolomiets, J.-M. Lehn, *Chem. Commun.* **2005**, 1519–1521; c) N. Giuseppone, J.-L. Schmitt, J.-M. Lehn, *Angew. Chem.* **2004**, *116*, 5010–5014; *Angew. Chem. Int. Ed.* **2004**, *43*, 4902–4906; d) J. R. Nitschke, *Angew. Chem.* **2004**, *116*, 3135–3137; *Angew. Chem. Int. Ed.* **2004**, *43*, 3073–3075; e) V. Goral, M. I. Nelen, A. V. Eliseev, J.-M. Lehn, *Proc. Natl. Acad. Sci. USA* **2001**, *98*, 1347–1352; f) D. M. Epstein, S. Choudhary, M. R. Churchill, K. M. Keil, A. V. Eliseev, J. R. Morrow, *Inorg. Chem.* **2001**, *40*, 1591–1596; g) F. Hof, C. Nuckolls, J. Rebek, Jr., *J. Am. Chem. Soc.* **2000**, *122*, 4251–4252.

[4] I. Huc, J.-M Lehn, *Proc. Natl. Acad. Sci. USA* **1997**, *94*, 2106–2110.

[5] P. T. Corbett, L. H. Tong, J. K. M. Sanders, S. Otto, *J. Am. Chem. Soc.* **2005**, *127*, 8902–8903.

[6] a) S. Hiraoka, Y. Kubota, M. Fujita, *Chem. Commun.* **2000**, 1509–1510; b) K. Severin, *Chem. Eur. J.* **2004**, *10*, 2565–2580; c) B. Saur, R. Scopelliti, K. Severin, *Chem. Eur. J.* **2006**, *12*, 1058–1066.

[7] M. Crego-Calama, Hulst, R. Fokkens, N. M. M. Nibbering, P. Timmerman, D. N. Reinhoudt, *Chem. Commun.* **1998**, 1021–1022.

[8] For a review about dynamic combinatorial chemistry that partially focuses on the difference between "classical" and dynamic combinatorial chemistry, see: J.-M. Lehn, *Chem. Eur. J.* **1999**, *5*, 2455–2463.

[9] a) P. T. Corbett, S. Otto, J. K. M. Sanders, *Chem. Eur. J.* **2004**, *10*, 3139–3143; b) Z. Grote, R. Scopelliti, K. Severin, *Angew. Chem.* **2003**, *115*, 3951–3955; *Angew. Chem. Int. Ed.* **2003**, *42*, 3821–3825; c) I. Saur, K. Severin, *Chem. Commun.* **2005**, 1471–1473; d) P. T. Corbett, J. K. M. Sanders, S. Otto, *J. Am. Chem. Soc.* **2005**, *127*, 9390–9392.

[10] S. L. Roberts, R. L. E. Furlan, S. Otto, J. K. M. Sanders, *Org. Biomol. Chem.* **2003**, *1*, 1625–1633.

[11] a) S. L. Roberts, R. L. E. Furlan, G. R. L. Cousins, J. K. M. Sanders, *Chem. Commun.* **2002**, 938–939; b) R. L. E. Furlan, Y.-F. Ng, G. R. L. Cousins, J. E. Redman, J. K. M. Sanders, *Tetrahedron* **2002**, *58*, 771–778; c) R. L. E. Furlan, Y.-F. Ng, S. Otto, J. K. M. Sanders, *J. Am. Chem. Soc.* **2001**, *123*, 8876–8877; d) G. R. L. Cousins, R. L. E. Furlan, Y.-F. Ng, J. E. Redman, J. K. M. Sanders, *Angew. Chem.* **2001**, *113*, 437–442; *Angew. Chem. Int. Ed.* **2001**, *40*, 423–428; e) R. L. E. Furlan, G. R. L. Cousins, J. K. M. Sanders, *Chem. Commun.* **2000**, 1761–1762; f) B. Hasenknopf, J.-M. Lehn, N. Boumediene, A. Dupont-Gervais, A. Van Dorsselaer, B. Kneisel, D. Fenske, *J. Am. Chem. Soc.* **1997**, *119*, 10956–10962; g) P. A. Brady, R. P. Bonar-Law, S. J. Rowan, C. J. Suckling, J. K. M. Sanders, *Chem. Commun.* **1996**, 319–320; h) B. Hasenknopf, J.-M. Lehn, B. O. Kneisel, G. Baum, D. Fenske, *Angew. Chem.* **1996**, *108*, 1987–1990; *Angew. Chem. Int. Ed. Engl.* **1996**, *35*, 1838–1840; i) O. Storm, U. Lüning, *Chem. Eur. J.* **2002**, *8*, 793–798; j) J. Leclaire, L. Vial, S. Otto, J. K. M. Sanders, *Chem. Commun.* **2005**, 1959–1961; k) K. R. West, K. D. Bake, S. Otto, *Org. Lett.* **2005**, *7*, 2615–2618; l) P. T. Corbett, L. H. Tong, J. K. M. Sanders, S. Otto, *J. Am. Chem. Soc.* **2005**, *127*, 8902–8903.

[12] a) B. Brisig, J. K. M. Sanders, S. Otto, *Angew. Chem.* ***2003***, *115*, 1308–1311; *Angew. Chem. Int. Ed.* **2003**, *42*, 1270–1273; b) Y. Kubota, S. Sakamoto, K. Yamaguchi, M. Fujita, *Proc. Natl. Acad. Sci. USA* **2002**, *99*, 4854–4856; c) S. Otto, R. L. E. Furlan, J. K. M. Sanders, *Science* **2002**, *297*, 590–593; d) S. Otto, R. L. E. Furlan, J. K. M. Sanders, *J. Am. Chem. Soc.* **2000**, *122*, 12063–12064; e) S. Otto, S. Kubik, *J. Am. Chem. Soc.* **2003**, *125*, 7804–7805.

[13] M. Crego-Calama, P. Timmerman, D. N. Reinhoudt, *Angew. Chem.* **2000**, *112*, 771–774; *Angew. Chem. Int. Ed.* **2000**, *39*, 755–758.

[14] a) Y. G. Ma, S. V. Kolotuchin, S. C. Zimmerman, *J. Am. Chem. Soc.* **2002**, *124*, 13757–13769; b) Z. Grote, R. Scopelliti, K. Severin, *Angew. Chem.* **2003**, *115*, 3951–3955; *Angew. Chem. Int. Ed.* **2003**, *42*, 3821–3825.

[15] P. Timmerman, R. H. Vreekamp, R. Hulst, W. Verboom, D. N. Reinhoudt, K. Rissanen, K. A. Udachin, J. Ripmeester, *Chem. Eur. J.* **1997**, *3*, 1823–1832.

[16] R. H. Vreekamp, J. P. M. van Duynhoven, M. Hubert, W. Verboom, D. N. Reinhoudt, *Angew. Chem.* **1996**, *108*, 1306–1309; *Angew. Chem. Int. Ed. Engl.* **1996**, *35*, 1215–1218.

[17] J. M. C. A. Kerckhoffs, F. W. B. van Leeuwen, A. L. Spek, H. Kooijman, M. Crego-Calama, D. N. Reinhoudt, *Angew. Chem.* **2003**, *115*, 5895–5900; *Angew. Chem. Int. Ed.* **2003**, *42*, 5717–5722.

[18] Here the amplified receptors are considered in principle as the best binders. Nevertheless, the amplification could be biased by the concentration of guest, see ref. [9]. Other experiments with different concentrations showed similar results. Furthermore, after templation by the guest only homomeric assemblies are formed, thus the libra-

ries are not biased by the experimental conditions otherwise the heteromeric assemblies would be preferred, see ref. [9b].

[19] In general, the signals observed in this solvent are sharper than those in $CDCl_3$. The shifts of the ^1H NMR signals for the encapsulation of **2a** by $\mathbf{1a}_3$·$(DEB)_6$ in $[D_8]$toluene differ slightly from those observed in $CDCl_3$.

[20] The signal labeled ■ in Figure 8b clearly comes from the homomeric complex $\mathbf{1a}_3$·$(DEB)_6$·$\mathbf{2a}_3$ as shown by the ^1H NMR spectrum of the individual assembly (Figure 8c). Integration of the signals reveals that those labeled with ▲ belong to one complex and those labeled with △ belong to another complex. The fact that three signals belong to one complex mean that these are heteromeric assemblies that give separate signals for each OH^n. The signals labeled with ▲ probably belong to complex $\mathbf{1a}_2$·$\mathbf{1c}_1$·$(DEB)_6$·$\mathbf{2a}_3$ when considering that OH^n protons closer to calix[4]arene melamine **1a** resonate at $\delta => 10.0$ ppm and the that OH^n protons closer to calix[4]arene melamine **1c** resonate at $\delta =< 9.9$ ppm. By applying the same reasoning, the signals labeled with △ belong to complex $\mathbf{1a}_1$·$\mathbf{1c}_2$·$(DEB)_6$·$\mathbf{2a}_3$. Consequently, it seems that calix[4]arene dimelamine **1c** in the dynamic mixture forms heteromeric complexes that are similar to complex $\mathbf{1a}_3$·$(DEB)_6$·$\mathbf{2a}_3$.

[21] See the Supporting Information for similar results obtained after addition of **2a** to DCL $\mathbf{1a}_2$·$\mathbf{1d}_1$·$(DEB)_6$.

[22] As previously published, this receptor can template the formation of noncovalent trimers $\mathbf{2a}_3$ and $\mathbf{2b}_3$ (see ref. [17]).

[23] Complex $\mathbf{1a}_3$·$(DEB)_6$·$\mathbf{2b}_3$ does not contain the OH^m proton and therefore the abundance of this complex could not be determined by the integration of this signal. Integration of the OH^n signals is difficult because these signals partially overlap.

[24] K. A. Jolliffe, M. Crego-Calama, R. Fokkens, N. M. M. Nibbering, P. Timmerman, D. N. Reinhoudt, *Angew. Chem.* **1998**, *110*, 1294–1297; *Angew. Chem. Int. Ed.* **1998**, *37*, 1247–1251.

[25] P. Timmerman, K. A. Jolliffe, M. Crego-Calama, J.-L. Weindmann, L. J. Prins, F. Cardullo, B. H. M. Snellink-Ruel, R. Fokkens, N. M. M. Nibbering, S. Shinkai, D. N. Reinhoudt, *Chem. Eur. J.* **2000**, *6*, 4104–4115.

[26] The amount of **2d** weighed was 3.8 equiv, but not all material dissolved in $CDCl_3$.

[27] F. Cardullo, M. Crego-Calama, B. H. M. Snellink-Rüel, J.-L. Weidmann, A. Bielejewska, R. Fokkens, N. M. M. Nibbering, P. Timmerman, D. N. Reinhoudt, *Chem. Commun.* **2000**, 367–368.

Received: August 17, 2006
Published online: December 1, 2006

